Smart Design Policies

Original scientific paper

2026, Volume 3, Number 1, pages 29–44

Satellite-Based Assessment of Vegetation Dynamics and their Potential Drivers in Lochinvar National Park Using Google Earth Engine

[1] **Grace Viswamo,** [2] **Timothy Mwaanga,** [3] **Musoka Nyongolo,** * [4] **Penjani H. Nyimbili,** [5] **Masauso Sakala,** [6] **Anastasia Kilundo,** and [7] **Erastus M. Mwanaumo**

[1, 2, 3, 4 & 5] Department of Geomatic Engineering, School of Engineering, University of Zambia, Zambia
[6] Department of National Park and Wildlife (DNPW), Ministry of Tourism and Arts, Zambia
[7] Department of Civil and Environmental Engineering, School of Engineering, University of Zambia, Zambia
[3, 4 & 7] National Centre for Uncrewed Aircraft Systems (NACUAS), University of Zambia, Zambia
[4 & 7] Built Environment and Information Technology, Faculty of Engineering, Walter Sisulu University, South Africa
[1] E-mail: *graceviswamo@gmail.com* , [2] E-mail: *timothymwaanga01@gmail.com* , [3] E-mail: *musokany-ongolo@gmail.com* ,
[4] E-mail: *penjani.nyimbili@unza.ac.zm* , [5] E-mail: *masauso.sakala@unza.ac.zm* , [6] E-mail: *anastaciakilundo@gmail.com* , [7] E-mail: *erastus.mwanaumo@unza.ac.zm*
[1] ORCID: *https://orcid.org/0009-0003-8509-3372* , [2] ORCID: *https://orcid.org/0009-0008-5102-9096* , [3] ORCID: *https://orcid.org/0009-0008-6732-0654* , [4] ORCID: *https://orcid.org/0000-0001-8271-5269* , [5] ORCID: *https://orcid.org/0009-0008-1679-4569* , [6] ORCID: *https://orcid.org/0009-0002-3185-3092* ,
[7] ORCID: *https://orcid.org/0000-0002-2911-3207*

ARTICLE INFO:
Received: 15 June 2026
Revised: 6 August 2026
Accepted: 13 August 2026
Available online: 15 August 2026

Keywords:
Remote Sensing, Google Earth Engine, NDVI, Land Cover Change, Wetland Conservation Policy.

ABSTRACT

This study examines vegetation dynamics and their potential environmental drivers in Lochinvar National Park, Zambia, over a 41-year period (1984 to 2025), using Landsat imagery processed on Google Earth Engine (GEE). The specific objectives were to: (1) quantify long-term land-cover change across six classes, namely water, grassland, woodland, floodplain, Mimosa pigra, and mine area; (2) characterise vegetation greenness trends using the Normalized Difference Vegetation Index (NDVI); and (3) examine the spatial association between these changes and hydrological alteration, invasive species spread, and human activity. The guiding research question was: how have vegetation cover and greenness in Lochinvar National Park changed since 1984, and to what extent are these changes spatially associated with hydrological, biological, and anthropogenic pressures? Using a Random Forest classifier (500 trees) applied to nine dry-season composite periods, grassland increased from 161.85 km² (39.31%) in 1984-1988 to 185.21 km² (44.99%) in 2024-2025, a net gain of 23.36 km² (+5.68 percentage points), while floodplain area declined from 114.32 km² (27.77%) to 76.89 km² (18.68%), a net loss of 37.43 km² (-9.09 percentage points). Mimosa pigra extent fell from a peak of 42.05 km² (10.22%) in 1994-1998 to 31.87 km² (7.74%) by 2024-2025. Classification accuracy reached 92% overall in the final period. Maximum NDVI fluctuated between 0.385 and 0.447 across the record, with a shallow positive linear trend of approximately +0.0004 NDVI units per year. These patterns are spatially consistent with, though not statistically proven to be caused by, altered flooding regimes downstream of the Itezhi-Tezhi and Kafue Gorge dams, sustained Mimosa pigra control efforts, and continued anthropogenic pressure. The study contributes an empirical, cloud-based monitoring framework that can inform smart, data-driven, and evidence-based land-management policy for wetland protected areas in Zambia and comparable floodplain systems in the region.

SMART DESIGN POLICIES (2026), 3(1), 29-44.
https://doi.org/10.38027/smart.v3n1-3

www.smartdpj.com

* Corresponding Author

How to cite this article: (APA Style)
Viswamo, G., Mwaanga, T., Nyongolo, M., Nyimbili, P. H., Sakala, M., Kilundo, A., & Mwanaumo, E. M. (2026). Satellite-based assessment of vegetation dynamics and their potential drivers in Lochinvar National Park using Google Earth Engine. *Smart Design Policies, 3*(1), 29-44. https://doi.org/10.38027/smart.v3n1-3

1. Introduction

1.1 Background and Ecological Context

Lochinvar National Park remains one of Zambia's most ecologically significant protected areas, renowned for its wetlands, floodplains, endemic wildlife, and exceptional birdlife, and is therefore vital for biodiversity conservation and ecological sustainability (Zambia Tourism, 2025). Over the past four decades, however, the park has faced mounting ecological pressure from natural and anthropogenic drivers, resulting in changes in vegetation structure and composition. Alteration of the natural flood cycle across the Kafue Flats, associated with the construction and operation of the Itezhi-Tezhi and Kafue Gorge dams, has been linked to uneven floodplain biomass productivity and vegetation responses among ecological zones (WWF Zambia, 2021; Mumba & Thompson, 2005). These hydrological changes have coincided with the spread of invasive shrub species, principally *Mimosa pigra* and *Dichrostachys cinerea*, which have encroached into termitaria grasslands and floodplain zones across eastern and southern Africa more broadly (Witt et al., 2020). This encroachment is associated with reduced plant species richness and altered soil nutrient balances, contributing to ecosystem instability (Shanungu, 2009; Kato-Noguchi, 2023). In addition, human activities, including illegal tree harvesting, cattle grazing, agricultural encroachment, and late burning, have been documented as contributing to habitat degradation in woodland areas adjacent to surrounding communities (Chomba & Wataru, 2014). These combined pressures underline the need for systematic, long-term monitoring of vegetation dynamics to support conservation and management interventions.

Remote sensing technologies, particularly when integrated with cloud-based platforms such as Google Earth Engine (GEE), provide an efficient means of monitoring environmental change over large spatial and temporal scales. Spectral vegetation indices such as the Normalized Difference Vegetation Index (NDVI) enable quantification of vegetation greenness and degraded areas with high spatial consistency (Roy et al., 2025). NDVI-based analysis is especially relevant in floodplain ecosystems, where vegetation dynamics are closely linked to seasonal hydrological variability. Several studies have demonstrated the effectiveness of NDVI-based and Random Forest approaches in assessing vegetation dynamics and land-cover change elsewhere: Li et al. (2022) examined growing-season vegetation coverage in the China-Myanmar Economic Corridor using GEE and a geographic detector model; Omar et al. (2022) applied GEE and multi-temporal Sentinel-2 imagery to assess vegetation dynamics and forest loss in Nigeria; Latifah et al. (2023) combined Random Forest and CA-Markov modelling for protected-forest land-cover change in Indonesia; and Matyukira and Mhangara (2023) used extreme gradient boosting, Random Forest, and fragmentation analysis to characterise landscape structural change in South Africa; and Li et al. (2023) applied Random Forest and extreme gradient boosting to monitor drought conditions in Southwest China from Landsat imagery. Collectively, these studies confirm the methodological maturity of GEE and Random Forest classification for vegetation monitoring, but none address a Zambian floodplain protected area over a four-decade record with an explicit, spatially mapped invasive-species class, which is the specific gap addressed here.

1.2 Conceptual Framework

This study is organised around three interacting pressure pathways through which vegetation composition in floodplain protected areas is understood to change. The first is the hydrological pathway, whereby altered flood timing, duration, and extent, arising from upstream and downstream water regulation, modify floodplain biomass productivity and the balance between floodplain, grassland, and woodland cover (Mumba & Thompson, 2005). The second is the biological invasion pathway, whereby *Mimosa pigra* exploits disturbed, seasonally inundated margins, forms dense monospecific stands, and displaces native floodplain and grassland vegetation, with cascading effects on habitat structure for wildlife (Witt et al., 2020; Kato-Noguchi, 2023). The third is the anthropogenic pathway, whereby illegal tree cutting, grazing, and fire directly remove or degrade woodland cover (Chomba & Wataru, 2014). These three pathways do not operate independently; for example, altered flooding can create the disturbed margins that facilitate *Mimosa pigra* establishment, while human pressure can be concentrated in areas made accessible by vegetation loss. This framework, rather than treating land-cover change as a single undifferentiated outcome, provides the analytical lens used in Section 4 to interpret the spatial and temporal classification and NDVI results, and to make explicit where the evidence supports an association between a pathway and an observed pattern, as opposed to where it does not.

1.3 Research Gap, Objectives, and Research Questions

Despite the methodological advances summarised above, wetland ecosystems such as the Kafue Flats continue to experience degradation from natural and anthropogenic factors, and systematic, long-term, spatially explicit monitoring of vegetation dynamics using satellite-based approaches remains limited specifically for Lochinvar National Park. Existing Zambian studies have either addressed a single driver in isolation, such as illegal harvesting (Chomba & Wataru, 2014) or invasive-species management (Shanungu, 2009), or have not extended the observation record across the multi-decadal span needed to separate short-term fluctuation from directional change. Furthermore, although GEE provides advanced capacity for processing large volumes of satellite data, its application to wetland monitoring in Zambia remains underutilised relative to comparable applications elsewhere (Li et al., 2022; Omar et al., 2022). This creates a specific gap in understanding the spatial and temporal pattern of vegetation change in Lochinvar National Park and the extent to which it coincides with hydrological, biological, and anthropogenic pressures.

This study addresses that gap through three objectives: (1) to quantify land-cover change in Lochinvar National Park between 1984 and 2025 across six mapped classes using a Random Forest classification of Landsat imagery on GEE; (2) to characterise long-term NDVI trends as an independent measure of vegetation greenness and condition; and (3) to assess the spatial and temporal association between observed vegetation change and hydrological alteration, *Mimosa pigra* expansion or contraction, and anthropogenic pressure. These objectives are addressed through the following research question: how have vegetation cover and greenness in Lochinvar National Park changed since 1984, and to what extent are these changes spatially associated with hydrological, biological, and anthropogenic pressures identified in the conceptual framework in Section 1.2?

1.4 Significance and Contribution to Smart, Data-Driven Conservation Policy

The significance of this research lies in its contribution to environmental monitoring and evidence-based conservation planning in wetland ecosystems, and, more specifically, to the smart design policy scope of this journal. Cloud-based geospatial platforms such as GEE allow environmental data to be processed, updated, and visualised at a scale and speed that supports data-driven and evidence-based land-management decision-making rather than periodic, resource-intensive field survey alone (Ghosh et al., 2022). This aligns directly with the broader smart land-use planning agenda, in which remote sensing, cloud computing, and structured monitoring indicators are positioned as core tools for evidence-based governance of land and natural resources (Cui et al., 2025; Juffe-Bignoli et al., 2024). By producing a repeatable, 41-year, spatially explicit record of land-cover and greenness change for a specific protected area, this study demonstrates a transferable monitoring framework that the Department of National Parks and Wildlife and comparable agencies could adopt as a standing, low-cost monitoring dashboard, informing where and when management interventions, such as targeted *Mimosa pigra* clearance or hydrological restoration advocacy, are most needed. The findings are intended to support the development of sustainable land-management strategies and to inform policy decisions aimed at preserving the ecological integrity of Lochinvar National Park and similar wetland environments in the region.

2. Materials and Methods

2.1 Study Area

Lochinvar National Park is located in the Southern Province of Zambia, along the southern edge of the Kafue Flats, with the Kafue River forming its northern boundary. The park covers an area of approximately 428 km² and is characterised by seasonally inundated floodplains in the northern section, extensive wetlands and grasslands, scattered termitaria zones, and woodland habitats predominantly in the southern region. The park supports large populations of the endemic Kafue lechwe (*Kobus leche kafuensis*) and over 420 bird species. Vegetation patterns are strongly influenced by seasonal flooding, with the northern floodplains inundated during the rainy season and the southern woodlands remaining relatively dry (Zambia Tourism, 2025).

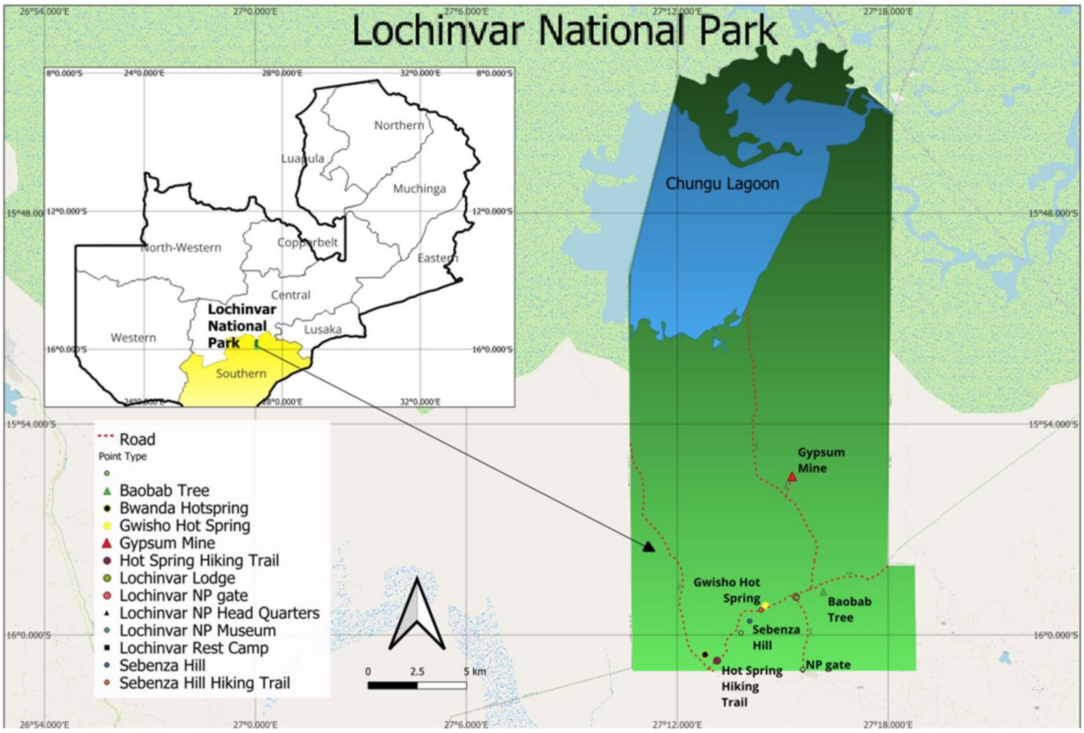

Figure 1. Study area: Lochinvar National Park, Southern Province, Zambia.

2.2 Methodological Framework

This study adopted an integrated remote sensing and geospatial analysis workflow, summarised under a single analytical framework in Figure 2, to assess long-term vegetation dynamics and their potential drivers in Lochinvar National Park using GEE. The framework groups the methods, techniques, and processing steps applied under four umbrellas: data acquisition and pre-processing, land-cover classification and change detection, accuracy assessment and driver association analysis, and data analysis and visualisation. Each umbrella is described in the corresponding subsection below.

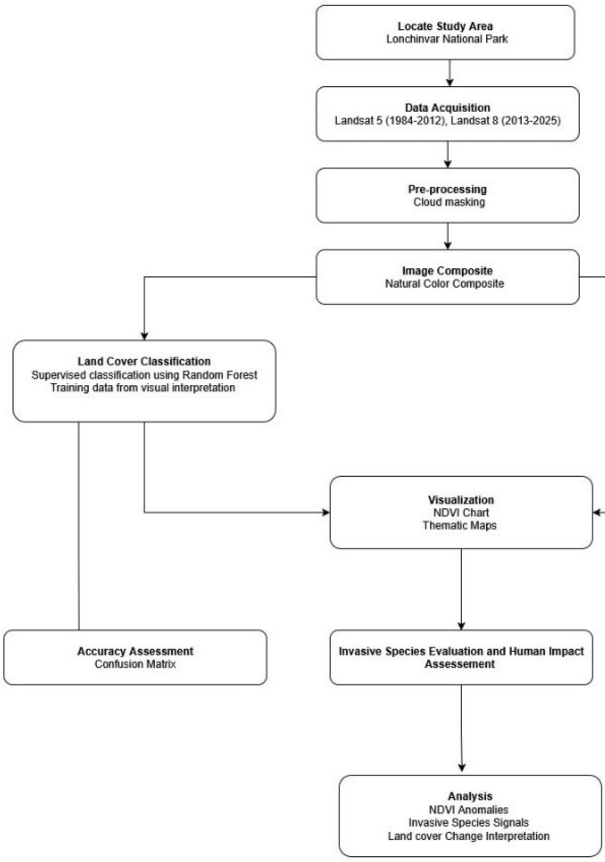

Figure 2. Methodological workflow (developed by the authors).

2.2.1 Data Acquisition and Pre-Processing

Satellite data were obtained from the GEE platform using Landsat 5 TM and Landsat 8 OLI surface reflectance datasets. These sensors were selected for their long-term temporal coverage and 30 m spatial resolution. Landsat 7 ETM+ imagery was deliberately excluded from the composite record: following the Scan Line Corrector failure in May 2003, Landsat 7 scenes contain systematic data gaps that introduce spatial inconsistency into pixel-based compositing and change detection, and its inclusion would have compromised the internal comparability of the record rather than improved it.

Landsat 5 imagery (1984-2011) and Landsat 8 imagery (2013-2025) were combined to create a continuous dataset spanning four decades. Because Landsat 5 and Landsat 8 differ in spectral response, a linear cross-sensor calibration was applied to NDVI values prior to compositing, following the cross-calibration approach documented for multi-sensor Landsat time series (Berner et al., 2023), so that apparent greenness change between sensors is not conflated with genuine vegetation change. Dry-season imagery was prioritised across all periods to reduce seasonal bias. A spatial boundary shapefile of Lochinvar National Park was created in QGIS and used as the region of interest to clip all imagery, and cloud-contaminated pixels were removed using QA_PIXEL and FMask quality bands.

Vegetation dynamics were assessed using NDVI, computed as (NIR - Red) / (NIR + Red) (Equation 1; Rouse et al., 1974), using Bands 4 and 3 for Landsat 5 and Bands 5 and 4 for Landsat 8. NDVI values range from -1.00 to +1.00 (Rahmi et al., 2024); water, snow, and cloud typically yield negative values, bare soil and built surfaces yield values near zero, and vegetation yields values from approximately 0.30 to +1.00 depending on density and health (Gandhi et al., 2015).

Median NDVI composites were generated for nine periods: 1984-1988, 1989-1993, 1994-1998, 1999-2003, 2004-2008, 2009-2013, 2014-2018, 2019-2023, and 2024-2025. The five-year window was chosen to balance two competing constraints: it is long enough to accumulate sufficient cloud-free, dry-season Landsat 5 acquisitions over Zambia in the 1980s and 1990s, when the archive is comparatively sparse, to form a reliable median composite, while remaining short enough to retain decadal-scale sensitivity to change, consistent with multi-year compositing windows used in comparable long-term Landsat vegetation studies (Latifah et al., 2023). The final period (2024-2025) spans two years only, reflecting the most recent dry-season imagery available at the time of analysis; this asymmetry is acknowledged as a limitation on the direct comparability of the final interval with the preceding five-year blocks and is revisited in Section 4.6.

2.2.2 Land Cover Classification and Change Detection

Land-cover classification was performed using a supervised Random Forest algorithm implemented in GEE, with 500 decision trees, selected for its robustness and demonstrated accuracy with high-dimensional remote sensing data. Six land-cover classes were mapped for every period: water, grassland, woodland, floodplain, *Mimosa pigra* (invasive species), and mine area, the last appearing only from the mid-1990s onward as gypsum extraction developed near the park boundary. This six-class scheme, rather than the narrower set used in earlier drafting of this study, is applied consistently across the methods and results reported here.

Training samples were digitised independently for each of the nine periods, using a stratified design proportional to the expected areal extent of each class, and cross-checked against Google Earth historical high-resolution basemap imagery and Landsat true-colour composites to maintain temporal consistency in spectral labelling. [Authors: insert the exact number of training polygons digitised per class per period from the GEE training-asset record.] A key methodological contribution of this study is the explicit mapping of *Mimosa pigra* as a dedicated land-cover class rather than an inferred category. Training data for this class were drawn from known infested areas, particularly around Chunga Lagoon and floodplain margins, and cross-referenced against Department of National Parks and Wildlife and WWF Zambia field monitoring records of *Mimosa pigra* infestation (Shanungu, 2009; WWF Zambia, 2021), rather than relying on spectral inference alone. Vegetation change detection combined NDVI differencing, time-series analysis, and post-classification comparison of the nine classified maps.

2.2.3 Accuracy Assessment

Accuracy assessment used a stratified random sampling design, with at least 50 independent validation points per land-cover class for each period. To reduce the circularity risk associated with using the same analyst and the same imagery interpretation logic for both training and validation, reference points were interpreted independently of the classification process by cross-referencing high-resolution historical basemap imagery not used during training-sample digitisation. Classification performance was evaluated using overall accuracy, producer's accuracy, user's accuracy, and the Kappa coefficient; the Kappa coefficient is reported alongside, rather than in place of, the full confusion matrix for each period, since Kappa alone can be an unreliable single indicator of classification quality (Feizizadeh et al., 2022). The final period (2024-2025) achieved an overall accuracy of 92%. [Authors: insert the full confusion matrix, producer's and user's accuracy, and Kappa coefficient for all nine periods.] The absence of independent field-based ground-truthing across the full four-decade record remains a limitation, discussed in Section 4.6.

2.2.4 Driver Association Analysis

To examine the potential drivers introduced in the conceptual framework (Section 1.2), spatial and temporal patterns derived from the NDVI series and classified maps were compared descriptively against independently documented records of hydrological operation, invasive-species management, and human pressure. Floodplain and grassland trends were compared against the operational history of the Itezhi-Tezhi and Kafue Gorge dams (Mumba & Thompson, 2005); the extent and timing of *Mimosa pigra* contraction after 2013 was compared against the documented timeline of control interventions led by the Department of National Parks and Wildlife and WWF Zambia (Shanungu, 2009; WWF Zambia, 2021; Floyd & Munenga, 2025); and woodland loss was compared against the documented pattern of illegal harvesting reported for the park (Chomba & Wataru, 2014). This analysis is explicitly descriptive and associative: it identifies temporal and spatial coincidence between mapped vegetation change and independently documented pressures, but it does not constitute a formal statistical attribution model, since the required rainfall, flood-extent, or socio-economic covariates were not available for inclusion in a multivariate model within the scope of this study. This limitation, and the corresponding recommendation for quantitative driver modelling in future work, is stated explicitly in Section 4.6 and Section 4.7.

2.2.5 Data Analysis and Visualisation

GEE tools were used to generate classified maps, NDVI composites, differencing maps, and the NDVI time-series chart. An ordinary least-squares linear regression was fitted to the nine-period maximum NDVI series to characterise the long-term trend (Figure 5). Because the underlying series is short (nine points) and shows non-monotonic, fluctuating behaviour rather than a smooth trend, a non-parametric Theil-Sen slope estimator with a Mann-Kendall significance test is recommended as a robustness check for the final submission, since these methods are less sensitive to the outlier-like peak recorded in 2009-2013 than ordinary least-squares regression (Wu et al., 2026). [Authors: insert the Theil-Sen slope, Mann-Kendall Z statistic, and associated p-value alongside the ordinary least-squares regression equation and R^2 value from the analysis output.]

3. Results

This section presents the findings of the satellite-based assessment of vegetation dynamics in Lochinvar National Park from 1984 to 2025. The results are organised into land-cover classification, classification accuracy, and NDVI analysis, and figures and tables are numbered sequentially in the order in which they are first cited.

3.1 Land Cover Classification Results

3.1.1 Land Cover Classification Maps

Land-cover classification was carried out for nine dry-season periods from 1984 to 2025 (Figure 3). Each panel (a-i) shows the six mapped classes: water, grassland, woodland, floodplain, *Mimosa pigra*, and mine area.

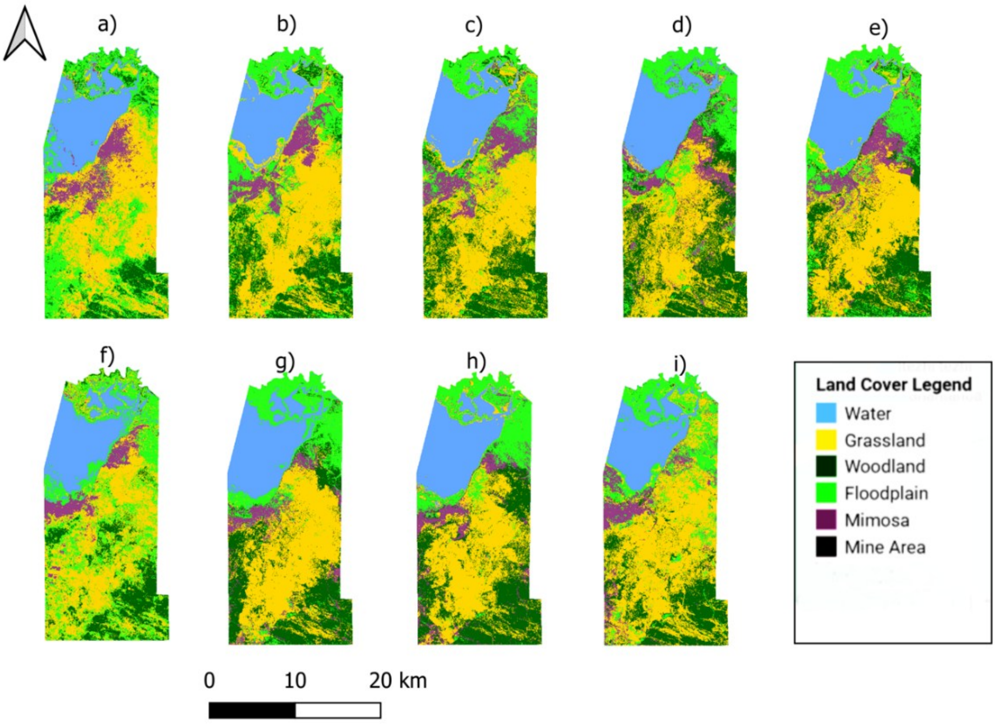

Figure 3. Five-year median classification composites for each time block: a (1984-1988), b (1989-1993), c (1994-1998), d (1999-2003), e (2004-2008), f (2009-2013), g (2014-2018), h (2019-2023), and i (2024-2025).

The classification maps show clear spatial change across the park over time. Grassland remained the dominant land cover throughout and expanded noticeably in the final years, particularly in the central and southern areas. Woodland cover fluctuated substantially, with denser patches in the southwestern and western zones during some periods, followed by fragmentation in later years. Floodplain vegetation varied across the eastern and northern lowland zones, contracting in some periods and expanding in others. *Mimosa pigra* persisted in scattered patches, particularly near wetland margins and floodplain edges. Water bodies remained relatively stable in location, though their extent varied slightly between periods. Mine areas were absent or negligible in the early years and became visible from 1994-1998 onward.

3.1.2 Land Cover Area and Percentage by Period

A summary of land-cover area and percentage across all nine study periods is presented in Table 1.

Table 1: Land cover area and percentage by period.

Period	Water (km^2)	Water (%)	Grassland (km^2)	Grassland (%)	Woodland (km^2)	Woodland (%)	Floodplain (km^2)	Floodplain (%)	Mimosa (km^2)	Mimosa (%)	Mine area (km^2)	Mine area (%)
1984-1988	79.07	19.21	161.85	39.31	38.71	9.40	114.32	27.77	35.00	8.50	0	0
1989-1993	68.39	16.61	166.98	40.56	76.25	18.52	85.52	20.78	31.81	7.73	0	0
1994-1998	72.53	17.62	159.54	38.75	88.29	21.45	66.54	16.16	42.05	10.22	0.04	0.001
1999-2003	80.74	19.61	132.48	32.18	106.76	25.93	71.88	17.46	37.09	9.01	0	0
2004-2008	76.15	18.50	146.97	35.70	84.99	20.65	81.23	19.73	39.61	9.62	0	0
2009-2013	76.11	18.49	149.06	36.21	58.14	14.12	122.14	29.67	23.49	5.71	0.12	0.029
2014-2018	81.08	19.69	150.04	36.45	92.95	22.58	77.39	18.80	27.50	6.68	0.12	0.029
2019-2023	81.32	19.75	141.68	34.42	106.20	25.80	68.31	16.59	31.45	7.64	0.14	0.035
2024-2025	66.47	16.15	185.21	44.99	68.52	16.64	76.89	18.68	31.87	7.74	0.018	0.047

Grassland increased from 161.85 km^2 (39.31%) in 1984-1988 to 185.21 km^2 (44.99%) in 2024-2025, a net gain of 23.36 km^2 (+5.68 percentage points). Woodland fluctuated, rising from 38.71 km^2 (9.40%) in the first period to a peak of 106.76 km^2 (25.93%) in 1999-2003 and 106.20 km^2 (25.80%) in 2019-2023, before contracting to 68.52 km^2 (16.64%) in the final period, a net change from the first to the last period of +29.81 km^2 (+7.24 percentage points). Floodplain coverage declined overall from 114.32 km^2 (27.77%) to 76.89 km^2 (18.68%), a net loss of 37.43 km^2 (-9.09 percentage points), though it peaked at 122.14 km^2 (29.67%) in 2009-2013. *Mimosa pigra* peaked at 42.05 km^2 (10.22%) in 1994-1998 and declined to 31.87 km^2 (7.74%) by 2024-2025, a net change from the first to the last period of -3.13 km^2 (-0.76 percentage points), with the more pronounced decline occurring after its 1994-1998 peak. Water bodies remained relatively stable, ranging from 66.47 km^2 to 81.32 km^2 across the record. Mine areas were negligible before 1994-1998 and increased slightly thereafter, reaching 0.14 km^2 (0.035%) by 2019-2023.

3.1.3 Classification Accuracy Assessment

Classification accuracy, assessed against independently interpreted stratified random reference points (Section 2.2.3), reached an overall accuracy of 92% in the final period (2024-2025). [Authors: insert the full accuracy table reporting overall accuracy, producer's accuracy, user's accuracy, and the Kappa coefficient for all nine periods, together with the corresponding confusion matrices, as Supplementary Table S2.] Preliminary visual review of the confusion patterns indicates that misclassification, where it occurs, is concentrated between spectrally similar classes, principally floodplain, grassland, and *Mimosa pigra* at their shared margins, which is consistent with the classification confusion documented for structurally similar wetland vegetation classes elsewhere (Latifah et al., 2023) and is addressed further as a limitation in Section 4.6.

3.2 NDVI Results

3.2.1 NDVI Composites and Time Series

NDVI composites were generated for nine dry-season periods to evaluate vegetation greenness, density, and condition (Figure 4). NDVI values in the study area ranged from approximately -0.024 to 0.437, where lower values (red tones) represent water, bare ground, or sparsely vegetated areas, moderate values (yellow tones) indicate mixed or stressed vegetation, and higher values (green tones) indicate healthier, denser vegetation.

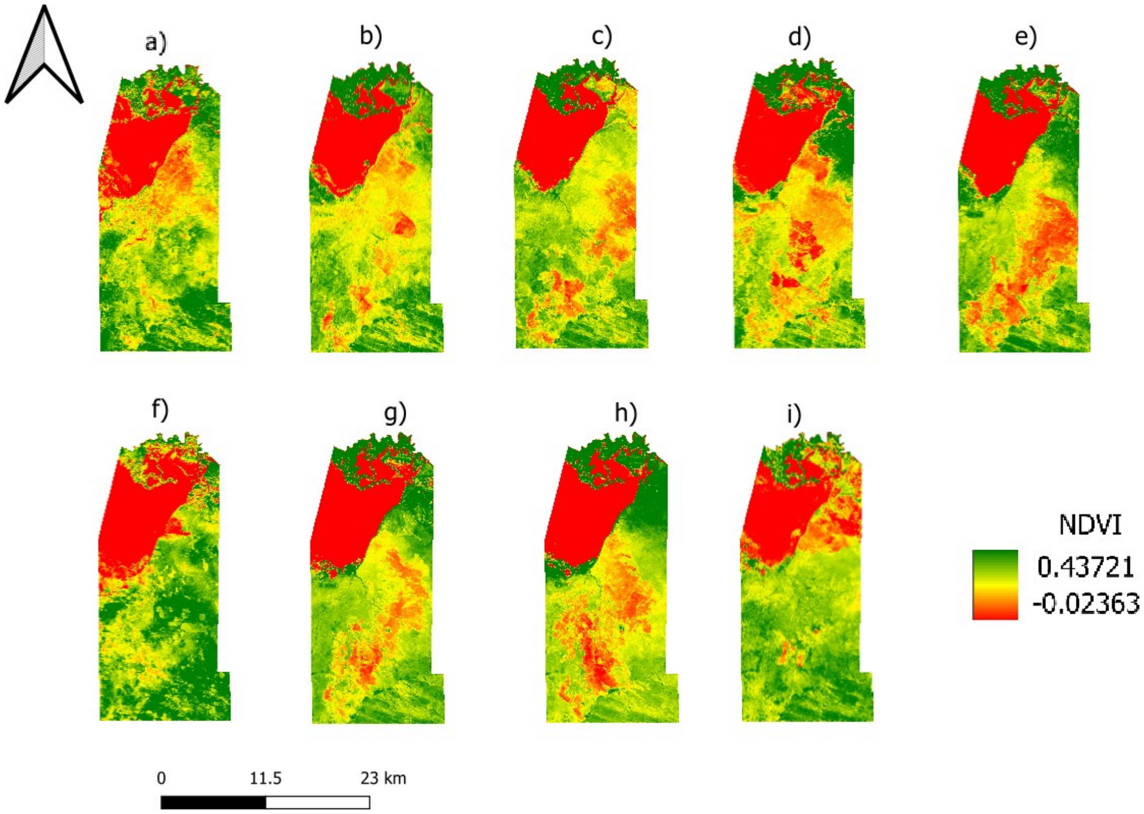

Figure 4. Five-year median NDVI composites for each time block: a (1984-1988), b (1989-1993), c (1994-1998), d (1999-2003), e (2004-2008), f (2009-2013), g (2014-2018), h (2019-2023), and i (2024-2025).

The 1984-1988 composite (Figure 4a) recorded a maximum NDVI of approximately 0.437, with extensive green patches across the southern and eastern areas. This was followed by a decline in 1989-1993 (Figure 4b) to about 0.392, then a modest recovery to approximately 0.410 in 1994-1998 (Figure 4c). Greenness declined again during 1999-2003 and 2004-2008 (Figure 4d-e), to approximately 0.385 and 0.387 respectively, with more fragmented vegetation patterns. The strongest vegetation conditions occurred in 2009-2013 (Figure 4f), with the highest recorded maximum NDVI of approximately 0.447. Maximum NDVI then declined to approximately 0.416 in 2014-2018 (Figure 4g), before stabilising at approximately 0.418 in 2019-2023 (Figure 4h) and 0.427 in 2024-2025 (Figure 4i).

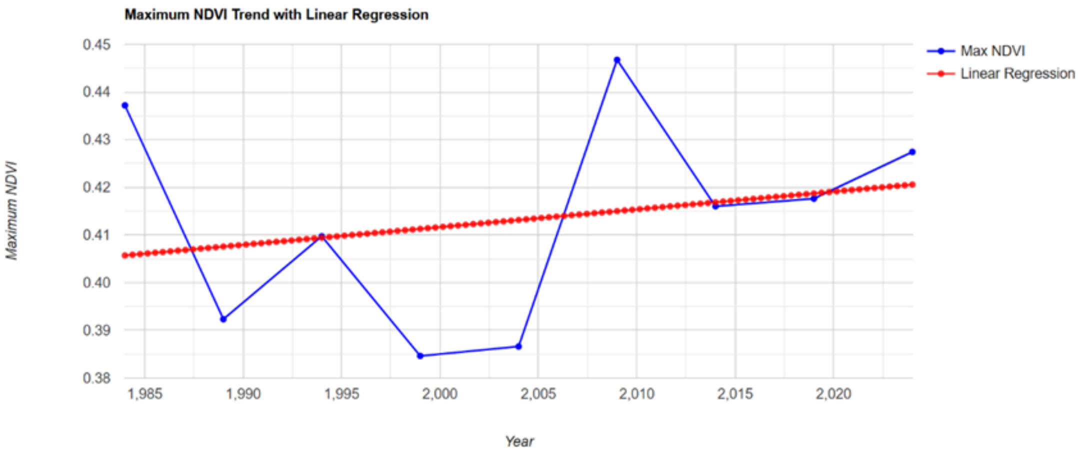

Figure 5. Maximum NDVI time series with linear regression trend, 1984-2025.

The NDVI time-series chart (Figure 5) confirms these fluctuations, showing alternating short-term increases and decreases across the study period, with a marked positive anomaly in 2009-2013. The fitted linear regression line rises from approximately 0.406 in 1984 to approximately 0.421 in 2024, corresponding to a shallow positive slope of approximately +0.0004 NDVI units per year, or a cumulative increase of roughly 0.015 NDVI units over the 40-year record. The total range of maximum NDVI values was relatively narrow (0.385-0.447), indicating that vegetation greenness remained broadly stable over the four decades, with recurring phases of stress and recovery rather than a dramatic directional shift in peak greenness.

3.2.2 NDVI Differencing

NDVI differencing was performed by subtracting consecutive composite images to detect vegetation change between periods. The resulting maps highlight areas of vegetation gain (green) and vegetation loss (purple) (Figure 6).

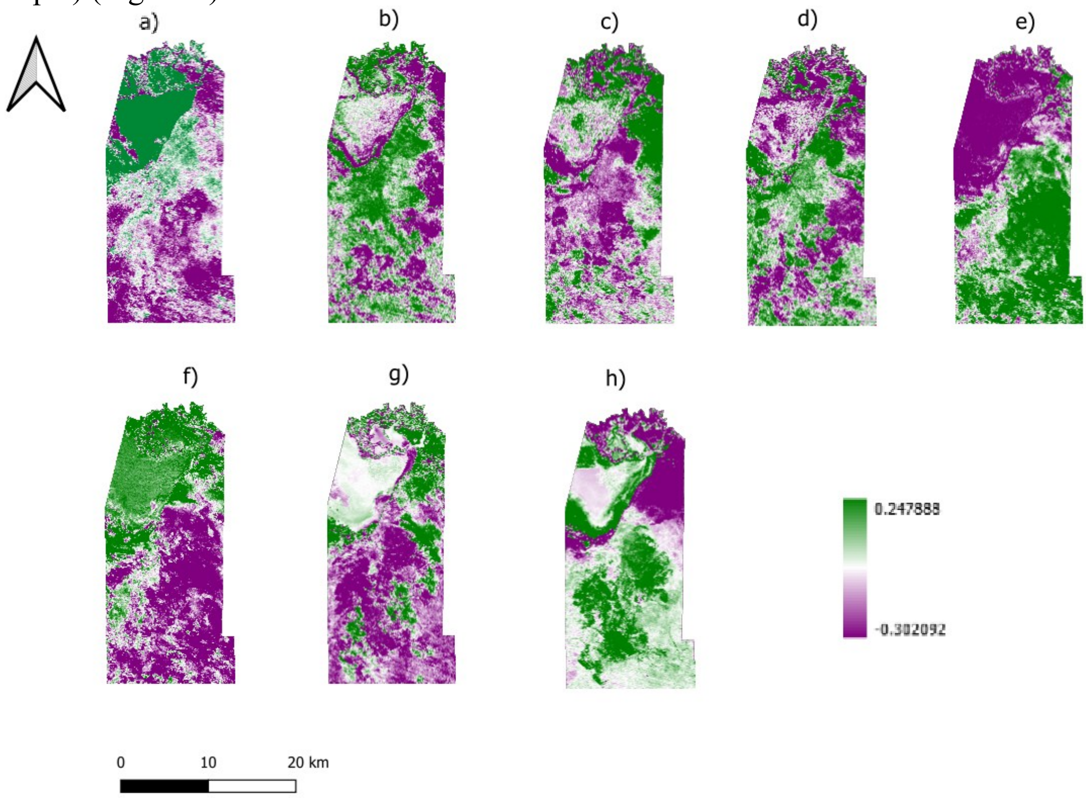

Figure 6. Five-year median NDVI differencing composites between successive time blocks: a (1984-1988 to 1989-1993), b (1989-1993 to 1994-1998), c (1994-1998 to 1999-2003), d (1999-2003 to 2004-2008), e (2004-2008 to 2009-2013), f (2009-2013 to 2014-2018), g (2014-2018 to 2019-2023), and h (2019-2023 to 2024-2025).

The transition from 1984-1988 to 1989-1993 (Figure 6a) shows widespread NDVI decline. Similar vegetation loss is visible from 1994-1998 to 1999-2003 (Figure 6c) and from 2009-2013 to 2014-2018 (Figure 6f), where purple tones dominate. In contrast, the intervals 2004-2008 to 2009-2013 (Figure 6e) and 2014-2018 to 2019-2023 (Figure 6g) show strong green signals, indicating widespread recovery. The final transition, 2019-2023 to 2024-2025 (Figure 6h), continues this recovery pattern.

4. Discussion

4.1 Overview of Vegetation Dynamics

Read against the conceptual framework in Section 1.2, the results indicate that vegetation change in Lochinvar National Park is not a simple linear process of loss or gain but a dynamic interplay of hydrological, biological, and anthropogenic pathways. Grassland increased steadily to 44.99% of the park by 2025, woodland fluctuated between approximately 9% and 26% across the record, floodplain coverage varied considerably in a pattern broadly consistent with hydrological conditions, and *Mimosa pigra* showed alternating phases of expansion and contraction consistent with the timing of documented control efforts. These patterns are consistent with the heterogeneous, alternating wet and dry character expected of semi-arid floodplain ecosystems and with prior work emphasising the sensitivity of wetland vegetation to both climatic variability and anthropogenic pressure, consistent with the broader relationship documented between NDVI and climatic variables in other seasonally variable landscapes (Mehmood et al., 2024).

4.2 Association with Hydrological Regime

Hydrology appears to be an important influence on floodplain vegetation distribution within the Kafue Flats. Floodplain area was largest during 2009-2013 (29.67%), the same period in which maximum NDVI also peaked, and smallest in the final period, 2024-2025 (18.68%). This pattern is spatially and temporally consistent with the documented alteration of natural flooding regimes by the Itezhi-Tezhi and Kafue Gorge dams (Mumba & Thompson, 2005), which is reported to disrupt the hydrological processes sustaining aquatic grasses and seasonal wetlands. The present study extends this understanding by providing a longer, spatially explicit record of how these hydrological changes coincide with measurable vegetation pattern across four decades; it does not, however, establish a formal causal or quantitative hydrological model linking reservoir operation records to vegetation response, and this distinction is maintained throughout this discussion in line with the associative framing set out in Section 2.2.4.

4.3 Invasive Species Dynamics

Mimosa pigra coverage reached its recorded peak of 10.22% in 1994-1998, a period plausibly associated with favourable hydrological conditions for seed dispersal and establishment along Chunga Lagoon. Once established, *Mimosa pigra* is documented to form dense thickets that outcompete native vegetation, alter soil nutrient cycling, and restrict wildlife movement (Braithwaite et al., 1989; Shanungu, 2009; Kato-Noguchi, 2023), and its distribution across eastern and southern Africa more broadly is associated with comparable socio-ecological impacts on grazing and fishing access (Witt et al., 2020). The decline in *Mimosa pigra* coverage after 2013, stabilising at approximately 7.74% by 2025, coincides temporally with control programmes implemented by WWF Zambia and the Department of National Parks and Wildlife (WWF Zambia, 2021; Floyd & Munenga, 2025). This temporal coincidence is consistent with, though it does not on its own confirm, the effectiveness of these interventions, since no management-performance dataset, such as recorded clearance area, follow-up survival rates, or cost data, was available for direct evaluation within this study; a formal evaluation against such a dataset is recommended as future work. Comparable integrated control programmes elsewhere, for example in Australia, have achieved sustained reductions in *Mimosa pigra* extent where mechanical, chemical, and biological control were combined with fire management (Paynter & Flanagan, 2004; Welgama et al., 2022), and the pattern observed in Lochinvar National Park is broadly consistent with that literature.

4.4 Ecological and Socio-Economic Implications

The observed vegetation dynamics carry plausible ecological and socio-economic implications, though these implications are inferred from land-cover pattern rather than measured directly. Grassland expansion may enhance forage availability for herbivores such as the Kafue lechwe but may also reduce woodland habitat important for bird species. The spread of *Mimosa pigra*, where it persists, is documented elsewhere to restrict grazing access, limit access to water resources, and reduce habitat suitable for fish breeding, with corresponding effects on communities that depend on the Kafue Flats for fishing and grazing (Witt et al., 2020). Because no household-level or livelihood survey data were collected as part of this remote-sensing study, these socio-economic implications are presented explicitly as inferences requiring dedicated field-based socio-economic data collection to confirm, rather than as findings of this study; this distinction addresses a specific methodological gap between the spatial evidence generated here and the socio-economic claims that such evidence can responsibly support.

4.5 Relevance to Smart, Data-Driven Conservation Policy

The findings support a specific, practical role for cloud-based remote sensing in smart, evidence-based land-management policy for protected wetland areas. A repeatable GEE-based monitoring workflow of the kind demonstrated here can function as a low-cost, standing indicator dashboard, comparable in principle to the systematic, repeatable, area-based conservation assessment approaches proposed for protected-area networks more broadly (Juffe-Bignoli et al., 2024) and to open-source, remote-sensing-based habitat condition methodologies developed to support conservation decision-making directly (Tough et al., 2025). Embedding such a dashboard within park management planning would allow the Department of National Parks and Wildlife to move from periodic, resource-intensive field assessment toward continuous, data-driven monitoring consistent with the smart land-use planning agenda (Cui et al., 2025; Ghosh et al., 2022), supporting more timely, spatially targeted decisions on where to prioritise *Mimosa pigra* clearance, woodland protection, or engagement with dam operators over environmental flow releases, in the same spirit as recent cloud-resilient, GEE-adjacent monitoring frameworks piloted for Zambian protected and peri-urban landscapes (Nyongolo et al., 2026).

4.6 Limitations of the Study

Several limitations should be acknowledged alongside the methodological refinements described in Section 2.2. The 30 m spatial resolution of Landsat imagery restricts detection of fine-scale vegetation change, particularly small or fragmented *Mimosa pigra* patches. Although cross-sensor calibration was applied (Section 2.2.1), residual differences between Landsat 5 and Landsat 8 spectral response cannot be entirely eliminated and may contribute a small amount of apparent trend that is not attributable to genuine vegetation change. Classification approach and training-sample availability may not be fully transferable across four decades of land-cover change, and confusion between spectrally similar classes, particularly floodplain, grassland, and *Mimosa pigra* at shared margins, is an acknowledged source of uncertainty (Section 3.1.3). The five-year compositing window, while justified in Section 2.2.1, necessarily smooths within-period variability, and the shortened final period (2024-2025) is not directly comparable in temporal length to the preceding blocks. Despite an overall classification accuracy of 92% in the final period, the absence of extensive field-based ground-truthing across the full historical record introduces uncertainty that only future field validation can resolve. Finally, the driver association analysis in Section 2.2.4 is descriptive rather than a formal statistical attribution model, since rainfall, flood-extent, and socio-economic covariates were not available for inclusion within the scope of this study.

4.7 Contribution and Future Research

This study contributes a 41-year, spatially explicit, six-class land-cover and NDVI record for a Zambian wetland protected area, integrating an explicit, independently verified *Mimosa pigra* class rather than treating invasive-species extent as an inferred outcome of other land-cover change. Methodologically, it demonstrates cross-sensor calibrated Landsat compositing on GEE as a transferable, low-cost workflow for data-scarce, multi-decadal wetland monitoring, and it makes explicit, rather than assumes, the distinction between spatially associative evidence and formal causal attribution when interpreting hydrological, biological, and anthropogenic drivers. This distinction is itself a methodological contribution relevant to remote-sensing-based conservation studies more broadly, where driver claims are not infrequently overstated relative to the underlying evidence.

Future research should prioritise four extensions: first, incorporation of higher-resolution satellite data and field-based ground-truthing to improve fine-scale classification accuracy and validate the confusion patterns identified in Section 3.1.3; second, integration of quantitative hydrological, climatic, and socio-economic covariates, including reservoir release records, rainfall, and household-level livelihood data, to move the driver association analysis in Section 2.2.4 toward a formal multivariate attribution model; third, application of non-parametric trend methods, such as Theil-Sen and Mann-Kendall, alongside predictive scenario modelling, to assess likely vegetation trajectories under continued hydrological regulation and climate variability; and fourth, formal evaluation of *Mimosa pigra* management-programme performance against a documented clearance and follow-up dataset, to test directly the association proposed in Section 4.3. Embedding the resulting workflow within a standing, park-level monitoring dashboard, as discussed in Section 4.5, would support more proactive and adaptive management of Lochinvar National Park and comparable protected wetland systems.

5. Conclusions

This study set out to quantify land-cover and NDVI change in Lochinvar National Park between 1984 and 2025 and to assess the spatial association between that change and hydrological, biological, and anthropogenic pressures. The evidence supports three main findings in relation to that objective. First, grassland expanded by 23.36 km² (+5.68 percentage points) and floodplain contracted by 37.43 km² (-9.09 percentage points) over the study period, while woodland fluctuated markedly rather than declining monotonically, indicating a dynamic rather than a uniformly degrading landscape. Second, *Mimosa pigra* extent declined from its 1994-1998 peak of 10.22% to 7.74% by 2024-2025, a pattern temporally consistent with documented control interventions, though not independently confirmed by a management-performance dataset. Third, maximum NDVI fluctuated within a comparatively narrow range (0.385-0.447) with only a shallow positive long-term trend, indicating that overall vegetation greenness has remained broadly stable despite marked within-record variability.

The study contributes to the existing literature in two specific ways. Empirically, it provides the first 41-year, spatially explicit, six-class land-cover and NDVI record for Lochinvar National Park that maps *Mimosa pigra* as an explicit, independently verified class rather than an inferred category, extending prior Zambia-focused work that addressed single drivers in isolation (Chomba & Wataru, 2014; Shanungu, 2009). Methodologically, it demonstrates a cross-sensor calibrated, GEE-based monitoring workflow, and it deliberately separates descriptive, spatially associative evidence from formal causal attribution when discussing hydrological, biological, and anthropogenic drivers, a distinction proposed here as good practice for remote-sensing-based conservation studies generally. Consistent with the smart design policy scope of this journal, the study further demonstrates how a repeatable, cloud-based monitoring workflow of this kind can support data-driven, evidence-based land-management decision-making by protected-area agencies, complementing rather than replacing periodic field assessment.

On this basis, the study supports targeted, evidence-based interventions, including continued and formally evaluated *Mimosa pigra* control, woodland protection in areas identified as subject to repeated illegal harvesting, and engagement with dam operators regarding environmental flow releases to the Kafue Flats. Institutionalising a GEE-based monitoring workflow of the kind demonstrated here within park management planning would support continuous, adaptive decision-making rather than periodic assessment alone.

Future research should extend this record with field-based ground-truthing, quantitative hydrological and socio-economic covariates, non-parametric trend analysis, and a formal evaluation of invasive-species management performance, as detailed in Section 4.7, in order to move from the spatially associative evidence presented here toward a more fully attributive understanding of the drivers of vegetation change in Lochinvar National Park.

Acknowledgements
We would like to express our sincere gratitude to everyone who contributed to the successful completion of this research project. We extend our profound appreciation to the University of Zambia for providing the resources, facilities, and academic environment necessary for this research. We are indebted to our supervisors, Dr. P. H. Nyimbili and Mr. M. Sakala, for their guidance, support, and mentorship throughout this research; their insights and feedback significantly shaped the direction and quality of this work. Our thanks also go to the Department of National Parks and Wildlife for providing essential data and information about Lochinvar National Park. Finally, we extend our gratitude to our families and friends for their support and encouragement throughout this research.

Funding
This research received no specific grant from any funding agency in the public, commercial, or not-for-profit sectors.

Conflicts of Interest
The authors report no conflicts of interest.

Data Availability Statement
All data generated or analysed during this study, including the GEE classification and NDVI scripts, are included in this article and its supplementary files, or are available from the corresponding author upon reasonable request.

Institutional Review Board Statement
The research involved publicly available satellite datasets and secondary documentary sources and therefore did not require ethical approval.

CRediT Author Statement
Timothy Mwaanga: Conceptualisation; Methodology; Data curation; Formal analysis; Investigation; Visualisation; Writing – Original Draft. Grace Viswamo: Methodology; Software; Data curation; Validation; Writing – Review & Editing. Musoka Nyongolo: Data curation; Formal analysis; Writing – Review & Editing. Penjani H. Nyimbili: Supervision; Methodology; Writing – Review & Editing. Masauso Sakala: Supervision; Validation; Writing – Review & Editing. Anastacia Kilundo: Project Administration; Validation. Erastus M. Mwanaumo: Project Administration, Validation, Resources. All authors have read and approved the final version of the manuscript.

References

Berner, L. T., Assmann, J. J., Normand, S., & Goetz, S. J. (2023). 'LandsatTS': An R package to facilitate retrieval, cleaning, cross-calibration, and phenological modeling of Landsat time series data. *Ecography*, 2023(9), e06768. https://doi.org/10.1111/ecog.06768

Braithwaite, R. W., Lonsdale, W. M., & Estbergs, J. A. (1989). Alien vegetation and native biota in tropical Australia: The impact of Mimosa pigra. *Biological Conservation*, 48(3), 189-210. https://doi.org/10.1016/0006-3207(89)90118-3

Chomba, C., & Wataru, T. (2014). Does illegal harvesting of woody plants influence physiognomic status and woody vegetation dynamics in Lochinvar National Park? *Global Journal of Biology, Agriculture & Health Sciences*, 3(3), 265-284.

Cui, X., Huo, H., Li, F., de Vries, W. T., & Paudel, B. (2025). Smart land use planning: Hotspots and prospects. *Land*, 14(11), 2193. https://doi.org/10.3390/land14112193

Feizizadeh, B., Darabi, S., Blaschke, T., & Lakes, T. (2022). QADI as a new method and alternative to Kappa for accuracy assessment of remote sensing-based image classification. *Sensors*, 22(12), 4506. https://doi.org/10.3390/s22124506

Floyd, K. S., & Munenga, D. (2025). Control of an invasive plant, Mimosa pigra, on the Kafue Flats to restore critical habitat for wildlife and livestock grazing. *African Journal of Wildlife Research*, 55(3). https://doi.org/10.3957/056.055.0342

Gandhi, G. M., Parthiban, S., & Thummalu, N. (2015). NDVI: Vegetation change detection using remote sensing and GIS, a case study of Vellore District. *Procedia Computer Science*, 57, 1199-1210. https://doi.org/10.1016/j.procs.2015.07.415

Ghosh, S., Kumar, D., & Kumari, R. (2022). Cloud-based large-scale data retrieval, mapping, and analysis for land monitoring applications with Google Earth Engine (GEE). *Environmental Challenges*, 9, 100605. https://doi.org/10.1016/j.envc.2022.100605

Juffe-Bignoli, D., Mandrici, A., Delli, G., Niamir, A., & Dubois, G. (2024). Delivering systematic and repeatable area-based conservation assessments: From global to local scales. *Land*, 13(9), 1506. https://doi.org/10.3390/land13091506

Kato-Noguchi, H. (2023). Invasive mechanisms of one of the world's worst alien plant species Mimosa pigra and its management. *Plants*, 12(10), 1960. https://doi.org/10.3390/plants12101960

Latifah, S., Akhsani, F., Sofiana, E. I., & Ferdiansah, M. R. (2023). Land cover change assessment using Random Forest and CA-Markov from remote sensing images in protected forest areas. *Remote Sensing Applications: Society and Environment*, 31, 101061. https://doi.org/10.1016/j.rsase.2023.101061

Li, J., Wang, J., Zhang, J., Liu, C., He, S., & Liu, L. (2022). Growing-season vegetation coverage patterns and driving factors in the China-Myanmar Economic Corridor based on Google Earth Engine and geographic detector. *Ecological Indicators*, 136, 108620. https://doi.org/10.1016/j.ecolind.2022.108620

Li, X., Jia, H., & Wang, L. (2023). Remote sensing monitoring of drought in Southwest China using Random Forest and extreme gradient boosting methods. *Remote Sensing*, 15(19), 4840. https://doi.org/10.3390/rs15194840

Matyukira, C., & Mhangara, P. (2023). Land cover and landscape structural changes using extreme gradient boosting, Random Forest and fragmentation analysis. *Remote Sensing*, 15(23), 5520. https://doi.org/10.3390/rs15235520

Mehmood, K., Anees, S. A., Muhammad, S., Hussain, K., Shahzad, F., Liu, Q., Ansari, M. J., Alharbi, S. A., & Khan, W. R. (2024). Analyzing vegetation health dynamics across seasons and regions through NDVI and climatic variables. *Scientific Reports*, 14. https://doi.org/10.1038/s41598-024-62464-7

Mumba, M., & Thompson, J. R. (2005). Hydrological and ecological impacts of dams on the Kafue Flats floodplain system, southern Zambia. *Physics and Chemistry of the Earth*, 30(6-7), 442-447. https://doi.org/10.1016/j.pce.2005.06.009

Nyimbili, P. H., Chalwe, N., Kawimbe, B. J., Lubilo, F., Mwanaumo, E. M., Thwala, W. D., & Erden, T. (2023). Quantifying the effect of the built environment on surface runoff using GIS and remote sensing: A case study of Ibex Hill-Lusaka. *Proceedings of the International Conference of Contemporary Affairs in Architecture and Urbanism-ICCAUA*, 6(1), 506-518. https://doi.org/10.38027/iccaua2023en0327

Nyongolo, M., Lubinda, F., Nyimbili, P. H., Nguvulu, A., Kilundo, A., & Mwanaumo, E. (2026). Cloud-resilient forest monitoring for sustainable urban land management: L-band SAR assessment of charcoal-driven peri-urban woodland change in Lusaka, Zambia. *Journal of Contemporary Urban Affairs*, 10(1), 282-295. https://doi.org/10.25034/ijcua.2026.v10n1-13

Omar, D., Idrees, M., Ahmadu, H., Yusuf, A., Ipadeola, O., Babalola, A., & Abdulyekeen, A. (2022). Assessment of vegetation dynamics and forest loss using Google Earth Engine and multi-temporal Sentinel-2 imagery. *Agro-Science*, 21(2). https://doi.org/10.4314/as.v21i2.10

Paynter, Q., & Flanagan, G. J. (2004). Integrating herbicide and mechanical control treatments with fire and biological control to manage an invasive wetland shrub, Mimosa pigra. *Journal of Applied Ecology*, 41(4), 615-629. https://doi.org/10.1111/j.0021-8901.2004.00931.x

Rahmi, M. A., Parikesit, P., & Withaningsih, S. (2024). Vegetation change analysis using Normalized Difference Vegetation Index (NDVI) in Sumedang Regency. *E3S Web of Conferences*, 495, 02007. https://doi.org/10.1051/e3sconf/202449502007

Rouse, J. W., Haas, R. H., Schell, J. A., & Deering, D. W. (1974). Monitoring the vernal advancement and retrogradation of natural vegetation. *NASA/GSFC Type III Final Report*, Greenbelt, Maryland.

Roy, S. K., Mojumder, P., Chowdhury, M., & Hasan, M. (2025). Evaluating mangrove forest dynamics and fragmentation in Sundarbans, Bangladesh using high-resolution Sentinel-2 satellite images. *Global Ecology and Conservation*, 58, e03493. https://doi.org/10.1016/j.gecco.2025.e03493

Shanungu, G. K. (2009). Management of the invasive Mimosa pigra L. in Lochinvar National Park, Zambia. *Biodiversity*, 10(2-3), 56-60. https://doi.org/10.1080/14888386.2009.9712844

Tough, L., Bamford, A., Harrison, A., Wood, K., Los, S., Van Biervliet, O., Turvey, S., & Duncan, C. (2025). An open source, remote sensing-based methodology for wetland habitat condition assessments to aid conservation decision-making. *Journal of Applied Ecology*, 62, 2844-2857. https://doi.org/10.1111/1365-2664.70135

Welgama, A., Florentine, S., & Roberts, J. (2022). A global review of the woody invasive alien species Mimosa pigra: Its biology and management implications. *Plants*, 11(18), 2366. https://doi.org/10.3390/plants11182366

Witt, A. B. R., Floyd, K. S., Nunda, W., Beale, T., Shanungu, G., & Kriticos, D. J. (2020). Mimosa pigra in eastern and southern Africa: Distribution and socio-ecological impacts. *Austral Ecology*, 45(7), 831-844. https://doi.org/10.1111/aec.12895

Wu, M., Huang, Z., Liu, S., Wu, Z., Hong, T., & Hu, X. (2026). Vegetation-cover change trends across different lengths of time series using NDVI: Contrasting Theil-Sen and Mann-Kendall with piece-wise regression. *Forests*, 17(5), 557. https://doi.org/10.3390/f17050557

WWF Zambia. (2021). Restoration of the Kafue Flats: For people and nature. https://wwfafrica.awsassets.panda.org/downloads/final_invasive_species___web.pdf

Zambia Tourism. (2025). Lochinvar National Park. https://www.zambiatourism.com/destinations/national-parks/lochinvar-national-park